

Comparative study of optical and magneto-optical properties of GdFe_2 and GdCo_2

This article has been downloaded from IOPscience. Please scroll down to see the full text article.

2007 J. Phys.: Condens. Matter 19 176203

(<http://iopscience.iop.org/0953-8984/19/17/176203>)

View [the table of contents for this issue](#), or go to the [journal homepage](#) for more

Download details:

IP Address: 129.252.86.83

The article was downloaded on 28/05/2010 at 17:53

Please note that [terms and conditions apply](#).

Comparative study of optical and magneto-optical properties of GdFe₂ and GdCo₂

Sapan Mohan Saini¹, Nirpendra Singh¹, Tashi Nautiyal¹ and Sushil Auluck^{1,2}

¹ Department of Physics, Indian Institute of Technology Roorkee, Roorkee 247667, India

² Institute Computer Center, Indian Institute of Technology Roorkee, Roorkee 247667, India

Received 30 November 2006, in final form 10 February 2007

Published 28 March 2007

Online at stacks.iop.org/JPhysCM/19/176203

Abstract

We report calculations of the optical and magneto-optical properties of GdFe₂ and GdCo₂ using the full-potential linear-augmented-plane-wave method. Calculations with the Coulomb corrected local spin density approximation (LSDA + *U*) give a better representation of the band structure, density of states and magnetic moments compared to LSDA alone. However, both LSDA and LSDA + *U* approximations give fairly good agreement with experiment for the diagonal optical conductivity. The calculated results for GdCo₂ are in better agreement with the 'oxide corrected' data. Our results suggest that the data for GdFe₂ are most likely influenced by surface oxidation, due to the high reactivity of these compounds. For the much smaller off-diagonal components and Kerr rotation, LSDA results are better than the LSDA + *U* results, particularly in the energy range 0–3 eV. We show that the unphysical negative ellipticity values are taken care of by the use of stronger relaxation, which also improves the qualitative agreement with experimental data. Overall we have obtained a fair agreement with the experimental data for both optical and magneto-optical properties. We feel that measurements over a larger energy range are required for facilitating an exhaustive and decisive comparison and also to strengthen the bond between theory and experiments.

1. Introduction

Rare-earth–transition-metal compounds have been studied intensively [1] because of their unique magnetic properties and useful technological applications as magneto-optical (MO) recording media. Among these, the study of GdFe₂ and GdCo₂ has attracted attention for the basic understanding of their electronic structure of rare-earth–transition-metal compounds. The optical and magneto-optical properties of Laves phases, RFe₂, have been measured by several groups [2–6]. Kravets *et al* [4] measured the optical conductivity spectra of RFe₂ (R = Gd, Ho, and Er) using a spectroscopic ellipsometer in the energy range 1–4 eV. Sharipov *et al* [5] measured the optical conductivity and magneto-optical Kerr effect (MOKE) of RFe₂ (R = Gd,

Tb, Dy, Ho, and Er) and YFe_2 and found that the optical conductivity spectra of RFe_2 are similar to that of YFe_2 , but the MO spectra were different. On the basis of their measurements, they concluded that the difference in the MO spectra of the various RFe_2 compounds is due to the 4f electrons. Lee *et al* [6] measured the diagonal and off-diagonal conductivity of RFe_2 ($\text{R} = \text{Gd, Tb, Ho, Lu}$) and GdCo_2 by applying a magnetic field of 0.5 T. They also measured the MOKE using a single crystal of RFe_2 with the same applied magnetic field, and observed that the single-crystal data show more features and larger magnitudes in the MOKE spectrum under the same experimental conditions than the polycrystalline data from both Katayama and Hasegawa [2] and Mukimov *et al* [3]. They also presented a calculation of the optical and MO properties of RFe_2 compounds using the tight-binding linear muffin-tin orbital (TB-LMTO) method under the LSDA, treating the 4f electrons of the rare earth as valence electrons [6]. Lee *et al* [7] measured the optical and magneto-optical constants of single-crystalline GdCo_2 by spectroscopic ellipsometry. They also studied the effect of oxidation of the sample surface on the optical data, as GdCo_2 is known to be quite reactive with oxygen [8, 9]. The measured data were corrected by considering the effect of a surface oxide layer on the sample, employing a three-phase model [10] in which the oxide layer was treated as being nonmagnetic and transparent. As the oxide thickness increases in the model, it is noticed that magnitude of the oxide-free optical conductivity deduced from the model becomes enhanced and the interband-transition structures of the off-diagonal components become more pronounced.

Besides the experimental and theoretical studies mentioned above, there have been several band structure calculations [11, 12] attempting to understand the magnetic properties of GdFe_2 . Brooks *et al* [11] calculated the electronic structure of RFe_2 ($\text{R} = \text{Gd-Lu}$) compounds treating the 4f electrons as part of a self-consistent outer core. Their calculated magnetic moments are in good agreement with measured values. They concluded that although the total conduction electron moment in RFe_2 compounds is largely independent of the R 4f spin, the ferromagnetic site-resolved moments change significantly. Tanaka *et al* [13] calculated the spin-polarized electronic structure of the amorphous alloy $\text{Gd}_{33}\text{Fe}_{67}$ and its crystalline phase. They concluded that the calculated density of states (DOS) in the amorphous phase shows good agreement with the experimental DOS observed by x-ray photoemission spectroscopy and is very different from that in the crystalline Laves phase. They attributed this difference to the different local atomic structure for the amorphous phase and the crystalline phase. Wu [14] calculated the DOS, magnetism and magnetostriction of GdFe_2 and GdCo_2 using the full-potential linear-augmented-plane-wave (FPLAPW) method, and treated the Gd 4f shell fully relativistically as core states, obtaining good agreement between calculated magnetostriction and the experimental data. Recently, Rhee [15] calculated the electronic structure and optical properties of GdFe_2 by using the FPLAPW method with the LSDA + U approximation, and concluded that LSDA + U improves the agreement between the experimental and calculated structural and magnetic properties. However, it produced a rather insignificant effect on the diagonal (σ_{xx}) and off-diagonal (σ_{xy}) spectra of GdFe_2 in the 1.5–5.5 eV range.

Though GdFe_2 and GdCo_2 have been studied in much detail for electronic structure and optical conductivity, to the best of our knowledge there has been hardly any calculation of their MO properties. We have tried to fill this void. We report a theoretical study of the optical and MO properties of GdFe_2 and GdCo_2 , studying the role of Fe/Co on these properties. We compare our results primarily with the recent data from [6, 7], which is for single crystals.

2. Details of calculations

Both GdFe_2 and GdCo_2 have the cubic Laves phase (C15) structure in which the Gd atoms are arranged in the diamond structure consisting of two fcc lattices displaced from each other

by one-fourth of a body diagonal and the transition-metal atoms are on sites of rhombohedral symmetry ($3m$) in a tetrahedral arrangement with four Gd atoms as the next neighbours. The equivalent Gd atoms are located at $(1/8, 1/8, 1/8)$, $(7/8, 7/8, 7/8)$ and Fe/Co atoms are at $(1/2, 1/2, 1/2)$, $(1/2, 3/4, 3/4)$, $(3/4, 3/4, 1/2)$, and $(3/4, 1/2, 3/4)$. GdFe₂ and GdCo₂ are ferrimagnetic, i.e. the magnetic moments of Fe/Co atoms align anti-parallel to those of Gd atoms. Spin-polarized calculations have been performed using the experimental lattice parameters [16]: 13.94 and 13.69 au for GdFe₂ and GdCo₂, respectively. The calculations have been performed using the full-potential linearized-augmented-plane-wave method as implemented in the WIEN2k code [17], within both the LSDA and LSDA + U approximations. The LSDA + U method explicitly includes the onsite Coulomb interaction term in the conventional Hamiltonian. There are various schemes for LSDA + U , of which we used the one introduced by Anisimov *et al* [18]. We have used $U = 6.7$ eV and $J = 0.7$ eV, as determined by Harmon *et al* [19] using the supercell approach for Gd. We used $R_{\text{mt}}K_{\text{max}}$ equal to 7.0, resulting in 2243 plane waves for the basis functions, and the cut-off energy is 7.84 Ryd. The basis functions, electron densities and potentials are calculated without any geometrical approximation. The \mathbf{k} -space integration was performed using the modified tetrahedron method [20]. Convergence with respect to energy, and the number of \mathbf{k} -points have been thoroughly checked. Self-consistency was obtained using 819 \mathbf{k} -points in the irreducible Brillouin zone (IBZ). Calculations for interband optical and magneto-optical properties have been carried out using a finer mesh of 1063 \mathbf{k} -points in the IBZ.

3. Results and discussion

The calculated band structures of GdX₂ ($X = \text{Fe}$ and Co) with the LSDA and LSDA + U are quite similar: the only differences are in terms of the shifting of f bands away from Fermi energy (E_{F}) when LSDA + U is used. Furthermore, the band structure of spin-up states is similar to that for spin-down states except that the spin-up Gd f bands are occupied and lie well below the E_{F} . The band structure of GdCo₂ using LSDA + U is shown in figure 1. The calculated spin-polarized band structure of GdCo₂ shows that the spin-down Gd f bands hybridize with the Gd p, d and Co p, spin-down states, while the spin-up Gd f bands remain unhybridized. Consequently, the width of Gd f bands is ~ 0.1 and ~ 0.4 eV for occupied and unoccupied states, respectively. These widths are almost the same as those for pure Gd (~ 0.2 and ~ 0.4 eV). The LSDA + U calculations show that the majority Gd f bands are centred around 7.5 eV below E_{F} , and the minority Gd f bands are centred around 3.5 eV above E_{F} in GdCo₂. Hence, the LSDA + U enhances the exchange splitting of the Gd f bands dramatically to ~ 11 eV (from ~ 5 eV with the LSDA), by pushing the 4f spin-up states much below E_{F} and 4f spin-down states well above the E_{F} . The f bands in the case of GdFe₂ and GdCo₂ are shifted slightly by ~ 0.5 eV for both the spins towards higher energies as compared to the f bands in pure Gd. Besides the Gd f states, there is a group of bands in the energy range from -4 to -2 eV mainly due to Co s, d and Gd d states. The bands from -2 to 2 eV are due to the hybridization of Co p, d and Gd p, d states. Above 2 eV, only Gd p and d states constitute the band structure. The total DOS (for all the atoms in the unit cell) along with partial d DOS (per atom) of GdFe₂ and GdCo₂ using the LSDA + U approximation is shown in figure 2. The DOS for spin-up and spin-down f bands is clearly identified as sharp outstanding peaks in the total DOS. The d states of Gd and Fe/Co dominate mainly in the energy range -3 to 3 eV and hence contribute significantly to the $N(E_{\text{F}})$.

In table 1 we summarize the values of $N(E_{\text{F}})$, magnetic moment (μ) and coefficient of electronic specific heat (γ) from this work and those obtained by various workers [14, 15] using the FPLAPW method. The calculated total magnetic moments of GdFe₂ and GdCo₂ are

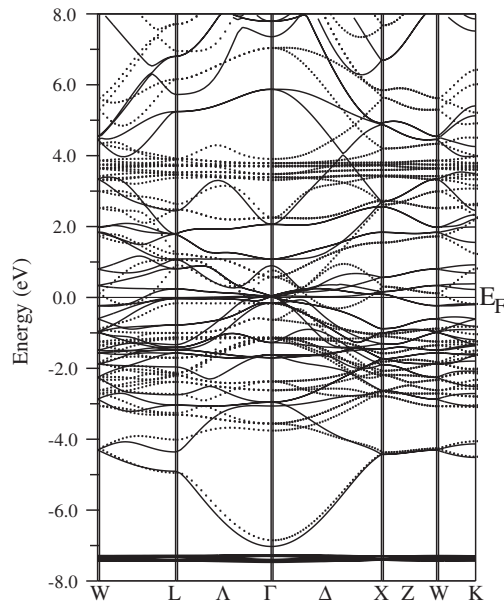


Figure 1. The band structure of GdCo₂ for spin-up (solid line) and spin-down (broken line) states using LSDA + *U*. The Fermi energy is labelled and marked with a faint horizontal line.

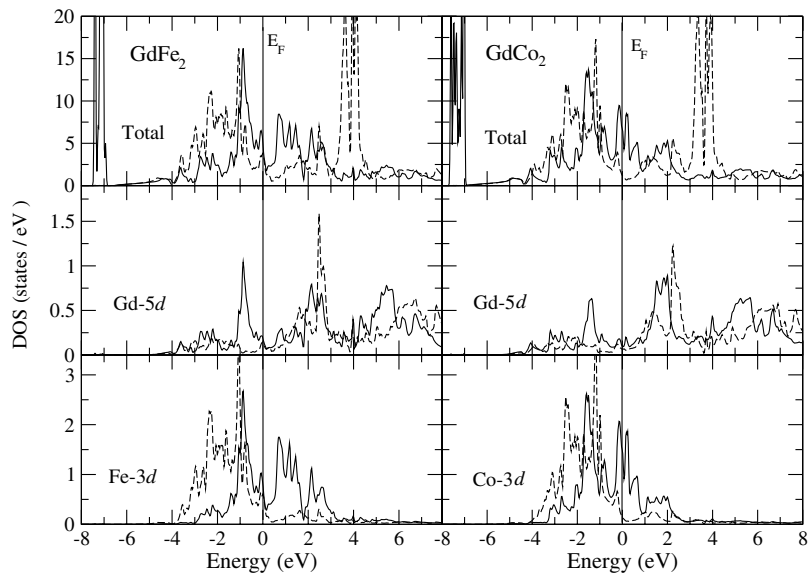


Figure 2. The total DOS (states/eV) of GdFe₂ and GdCo₂ for spin-up (solid line) and spin-down (broken line) states using LSDA + *U*, along with partial d DOS per atom for each kind. The vertical line marks the Fermi energy.

3.714 and 5.234 μ_B , respectively, in good agreement with experiment [6, 21]. We note that in GdFe₂, the value of magnetic moment at the Gd site (7.536 μ_B) is much closer to that in pure Gd (7.63 μ_B) and that of Fe also is very close to that of a pure Fe atom (2.21 μ_B). On the other

Table 1. Total and partial magnetic moment μ (in μ_B), coefficient of electronic specific heat γ (in $\text{mJ mol}^{-1} \text{K}^{-2}$), and density of states at the Fermi level $N(E_F)$ (in states/Ryd/spin/unit cell), for GdFe_2 and GdCo_2 from this work and Rhee [15] using LSDA + U , and from Wu [16] using Gd 4f states as core states, along with the experimental value for GdFe_2 [6] and GdCo_2 [21].

	GdFe ₂				GdCo ₂		
	Theory			Expt.	Theory		
	This work	Rhee	Wu		This work	Wu	Expt.
Total μ	3.714	3.385	3.85	3.46	5.234	4.99	5.3
μ_{Gd}	7.536	7.552	7.58		7.349	7.46	
μ_{Fe}	-2.05	-2.263	-1.96				
μ_{Co}					-1.18	-1.24	
μ_{int}	0.298	0.359			0.255		
$N(E_F)$		68.53				54.61	
γ		23.78				18.96	

hand, in GdCo_2 , the magnetic moment at the Gd site is $7.349 \mu_B$, showing a 4% drop, and that of Co shows even stronger impact dropping by $\sim 29\%$ in comparison to that in elemental Co ($1.66 \mu_B$) [22]. This suggests that the interatomic interactions in GdCo_2 are much stronger, and affect the Co atoms more, than in GdFe_2 . To get a better idea, we compared the d DOS of pure Co with that of Co in GdCo_2 and found that the d DOS of Co in GdCo_2 shows enhanced values for the occupied minority d DOS. This is due to the filling of the minority-spin d bands of Co by the conduction electrons from Gd atoms, in agreement with Huq [23]. This explains the reduction of the Co magnetic moment in GdCo_2 compared to that in pure Co. To the best of our knowledge there is no experimental value of electronic specific heat for GdFe_2 and GdCo_2 . We have obtained 23.78 and $18.96 \text{ mJ mol}^{-1} \text{K}^{-2}$, respectively, with LSDA + U .

To study the optical properties of GdFe_2 and GdCo_2 , we calculated the diagonal as well as off-diagonal components of the interband optical conductivity tensor. We tried various values of the broadening to simulate experimental broadening due to finite life-time effects: small values give a peaky spectrum while large values flatten the peaks, weakening the structures. All the results presented henceforth are for a moderate broadening of 0.6 eV . A comparison of σ_{1xx} for GdFe_2 and GdCo_2 reveals that the two are very similar, with almost the same peak positions and magnitude. Also these compounds exhibit much smaller anisotropy (i.e. $\sigma_{1xx} \approx \sigma_{1zz}$) as compared to hcp Gd [24]. Hence we have displayed only the σ_{1xx} , the absorptive component of diagonal optical conductivity, using the LSDA and LSDA + U approximations in figure 3. We note that the diagonal optical conductivity curves from the LSDA and LSDA + U are very similar for GdFe_2 as well as for GdCo_2 . Bearing in mind the dramatic shifting of the f states away from the Fermi level on inclusion of on-site Coulomb interactions with LSDA + U , this clearly indicates that the occupied Gd f states do not play an important role in the diagonal optical conductivity in the given energy range.

The upper half of the left panel in figure 3 shows the σ_{1xx} of GdFe_2 . The experimental spectrum is quite smooth, while calculations show a broad peak at $\sim 2.7 \text{ eV}$ with the LSDA and LSDA + U approximations. The magnitude of the calculated optical conductivity is almost double that obtained from experiment [6, 7]. Rhee's calculations also show a similar structure. This large magnitude could be attributed only partly to slight deviations from the sum rule for conductivity (i.e. $\int_0^\infty \sigma_1(\omega) d\omega = \frac{1}{2}\pi\omega_p^2$), and could be mainly due to the high reactivity of the surface of rare-earth compounds. The optical conductivity of GdCo_2 (the upper half of the right panel) confirms this reasoning. Along with calculated curves, we have also shown the measured

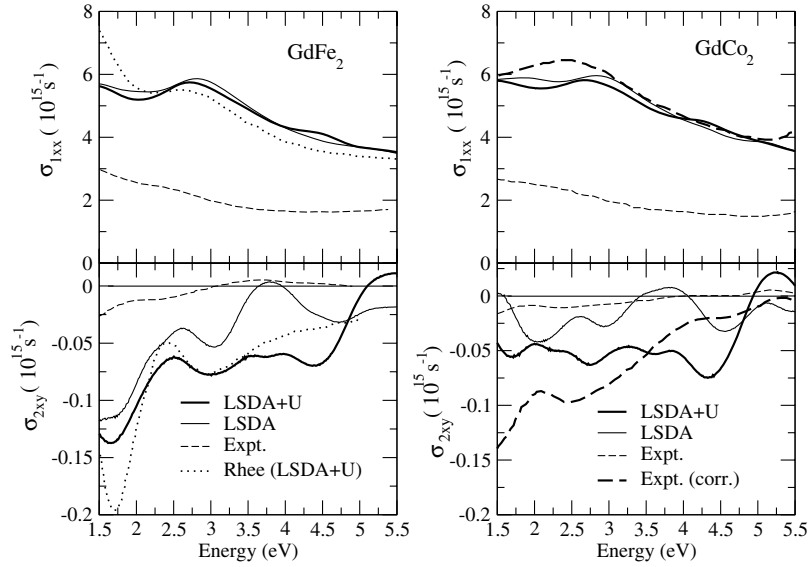


Figure 3. The diagonal (σ_{1xx}) and off-diagonal (σ_{2xy}) optical conductivity of GdFe_2 and GdCo_2 . The curve labelled as *expt.(corr.)* stands for experimental data corrected for surface oxidation.

values [6, 7], which originally are much lower as compared to calculated values. The measured values, when corrected by Lee *et al* [7] for surface oxidation, show a remarkable enhancement, bringing the calculated magnitudes of σ_{1xx} in very good agreement with experiment. The calculated σ_{1xx} of GdFe_2 and GdCo_2 are quite similar, and both LSDA and LSDA + U methods give good agreement with the experiments. The structure around 2.7 eV could be due to the transitions from occupied Fe/Co p, d states to unoccupied Gd p, d states.

The absorptive part, σ_{2xy} , of the off-diagonal conductivity is also presented in figure 3 (lower half), the left panel being for GdFe_2 and the right panel for GdCo_2 . The smaller magnitude of the off-diagonal conductivity offers a more stringent test to the theory and makes the differences amongst various calculations far more pronounced, as also the difference between calculations and experimental data. The experimental data for GdFe_2 are almost the same as the data for GdCo_2 without corrections for surface oxidation. The experimental data for GdFe_2 are smooth, producing an almost straight line which crosses the zero at 3 eV. The calculated spectra show relatively sharper features with sharper variations. Unlike the experiment, neither LSDA nor LSDA + U exhibits a change of sign at 3 eV. Considering the effect of a surface oxide layer on the sample leads to much enhanced values and brings the calculated magnitudes closer to the experimental data. The differences in our results and those from Rhee [15] can be attributed to different broadenings and to the adoption of different options for LSDA + U . Rhee [15] has used the ‘around-the-mean-field’ method introduced by Czyzyk and Sawatzky [25]. The lower half of the right panel for σ_{2xy} of GdCo_2 shows that the oxide-corrected spectrum shows relatively sharp features. Our LSDA + U results show a better agreement with data, though we obtain a smaller range of negative σ_{2xy} values. LSDA results seem less in agreement as compared to LSDA + U results.

Figure 4 displays the theoretical as well as the experimental Kerr rotation and Kerr ellipticity for GdFe_2 and GdCo_2 . Interestingly, the calculations overestimate the Kerr angle spectra, while the Kerr ellipticity is underestimated for both the compounds. The experimental curve [6, 7] shows that the Kerr angle stays small in GdFe_2 (left panel, upper half) reaching

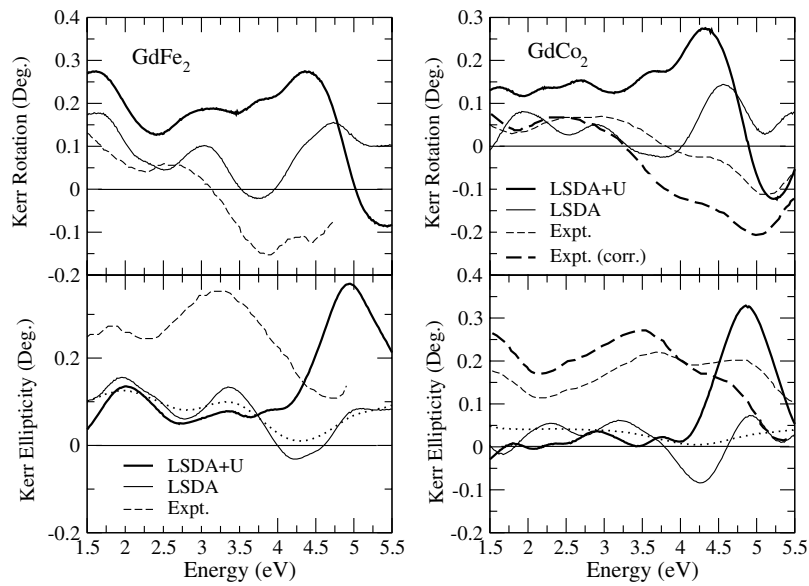


Figure 4. Kerr angle and Kerr ellipticity of GdFe_2 and GdCo_2 . The curve labelled as *expt.(corr.)* stands for experimental data corrected for surface oxidation. The dotted curves for ellipticity correspond to LSDA results with a stronger relaxation (1 eV for GdFe_2 and 1.5 eV for GdCo_2).

a maximum of only $\sim 0.15^\circ$ around 1.5 eV, and reaching $\sim -0.22^\circ$ in GdCo_2 (right panel, upper half) around 5 eV. Our calculated Kerr rotation, especially with the LSDA, shows similar trends as in the experimental data in the energy range 0–3 eV, though with somewhat enhanced magnitudes. It is worth mentioning at this point that the LSDA results of Oppeneer *et al* [26] for Kerr rotation and Kerr ellipticity of GdFe_2 are in agreement (apart from a shifting of the position of the structures) with the experimental data by Katayama and Hasegawa [2]. Since these data [2] are quite old as well as having been obtained on a polycrystalline sample, we compare our calculated Kerr rotation and Kerr ellipticity with recent single-crystal data of Lee *et al* [6], which give sharper structures. Our results are also in qualitative agreement with the data of Katayama and Hasegawa [2] and earlier calculations [26], except that we get negative values of Kerr rotation at high energies, in agreement with the recent data [6]. The negative values of the Kerr rotation are missing from the older reports [2, 26].

The calculated (LSDA and LSDA + U) Kerr ellipticity in GdFe_2 shows fair agreement with experiment at low energies, while at higher energies, the LSDA gives unphysical negative values. At low energies, the calculated (LSDA and LSDA + U) values for GdCo_2 are too small and also become negative. However, in the high-energy range (larger than 5 eV), the ellipticity increases, especially with LSDA + U . The calculated negative values of the ellipticity are quite unphysical, which could be attributed to the weak relaxation used in our calculations. Taking a stronger relaxation eliminates the negative ellipticity values, as shown for the LSDA results in figure 4, and also improves the qualitative agreement with experiment; however, the structures become less sharp.

4. Conclusions

We have performed spin-polarized full-potential calculations of the optical and magneto-optical properties for GdFe_2 and GdCo_2 using LSDA and LSDA + U approximations. We find a

shifting of majority as well as minority f bands away from Fermi level when LSDA + U is used, leading to a better representation for the DOS at the Fermi level. A comparison with experimental data for the optical conductivity suggests that both LSDA and LSDA + U approximations reproduce the diagonal part fairly well. We also note that the σ_{1xx} curves from LSDA and LSDA + U are very similar for GdFe₂ and GdCo₂. The LSDA + U method clearly indicates that the occupied Gd f states do not play an important role in the diagonal optical conductivity in the given energy range. The experimental curve of the off-diagonal part for both the compounds is almost flat with a faint shoulder, and our LSDA + U results show the slow variation and give better agreement with the experimental data. The calculated results for GdCo₂ are in better agreement with the 'oxide-corrected' data. Our results suggest that the data for GdFe₂ also appear to be influenced by surface oxidation, due to the high reactivity of these compounds. For the Kerr rotation of both the compounds, the LSDA shows similar trends as in the experiment up to 3 eV. The experimental Kerr ellipticity for both compounds has a positive value; both LSDA and LSDA + U yield much smaller magnitude and hence touch/cross the energy axis to give negative values. The unphysical negative ellipticity, however, is taken care of by the use of stronger relaxation, which also improves the qualitative agreement with experimental data. However, the sharpness of the structures diminishes. Overall we see that for low-magnitude off-diagonal optical conductivity and MOKE, the LSDA reproduces the experiments fairly well, particularly in the energy range 0–3 eV. Hence we obtain an overall fair agreement with the experimental data for both optical and magneto-optical properties. However, a better agreement between theory and experiment would be welcome. We feel that the range of experimental data is too small, and measurements over a larger range are required to facilitate a better and decisive comparison with the theory.

Acknowledgment

We gratefully acknowledge the support from the Department of Science and Technology (DST), India, through grant No. SP/S2/M-26/99, to carry out this work.

References

- [1] Buschow K H J 1980 *Ferromagnetic Materials* vol 1, ed E P Wohlfahrt (Amsterdam: North-Holland) p 297
- [2] Katayama T and Hasegawa Sendai K 1981 *Proc. 4th Int. Conf. on Rapidly Quenched Materials* p 915
- [3] Mukimov K M, Sharipov Sh M and Ernazarova L A 1985 *Phys. Status Solidi b* **127** K129
- [4] Kravets V G, Poperenko L V and Shaikevich I A 1988 *Izv. Vys. Ucheb. Ved. Fiz.* **12** 64
- [5] Sharipov Sh M, Mukimov K M, Ernazarova L A, Andereyev A V and Kudervatykh N V 1990 *Phys. Met. Metall.* **69** 50
- [6] Lee S J, Lange R J, Canfield P C, Harmon B N and Lynch D W 2000 *Phys. Rev. B* **61** 9669
- [7] Lee S J, Kim K J, Canfield P C and Lynch D W 2000 *J. Magn. Magn. Mater.* **213** 312
Lee S J and Kim K J 2001 *Solid State Commun.* **118** 269
- [8] Lee E W and Choudhury G M 1976 *J. Less-Common Met.* **46** 305
- [9] Shen D H, Mizokawa Y, Iwasaki H, Shen D F, Numata T and Nakamura S 1981 *Japan. J. Appl. Phys.* **20** L757
- [10] Azzam R A M and Bashara N M 1977 *Ellipsometry and Polarized Light* (Amsterdam: North-Holland)
- [11] Brooks M S S, Eriksson O and Johansson B 1989 *J. Phys.: Condens. Matter* **1** 5861
Brooks M S S, Nordstrom L and Johansson B 1991 *J. Phys.: Condens. Matter* **3** 2357
- [12] Coehoorn R 1989 *Phys. Rev. B* **39** 13702
Eriksson O, Nordstrom L, Brooks M S S and Johansson B 1988 *Phys. Rev. Lett.* **60** 2523
- [13] Tanaka H, Takayama S and Fujiwara T 1992 *Phys. Rev. B* **46** 7390
- [14] Wu R 1999 *J. Appl. Phys.* **85** 6217
- [15] Rhee J Y 2003 *J. Korean Phys. Soc.* **43** 792
- [16] Taylor K N R 1971 *Adv. Phys.* **2** 551

- [17] Blaha P, Schwarz K, Madsen G K H, Kvasnicka D and Luitz J 2001 *WIEN2k An Augmented Plane Wave +Local Orbitals Program for Calculating Crystal Properties* Techn. Universität Wien, Austria (ISBN 39501031-1-2)
- [18] Anisimov V I, Zaanen J and Andersen O K 1991 *Phys. Rev. B* **44** 943
Anisimov V I, Solovyev I V, Korotin M A, Czyzyk M T and Sawatzky G A 1993 *Phys. Rev. B* **48** 16929
- [19] Harmon B N, Antropov V P, Liechtenstein A I, Solovyev I V and Anisimov V I 1995 *J. Phys. Chem. Solids* **56** 1521
- [20] Von Barth U and Hedin L 1972 *J. Phys. C: Solid State Phys.* **5** 1629
- [21] Gignoux G, Givord F and Lemaire R 1975 *Phys. Rev. B* **12** 3878
- [22] Stearns M B 1986 *Numerical Data and Functional Relationships in Science and Technology (Landolt-Bornstein, New Series Group 3, vol 19, Part A)* ed H P J Wijn (Berlin: Springer)
- [23] Huq M 1982 *Phys. Status Solidi a* **74** 667
- [24] Saini S M, Singh N, Nautiyal T and Auluck S 2007 *J. Appl. Phys.* **101** 033522
Saini S M, Singh N, Nautiyal T and Auluck S 2006 *Solid State Commun.* **140** 125
- [25] Czyzyk M T and Sawatzky G A 1994 *Phys. Rev. B* **49** 14211
- [26] Oppeneer P M 2001 *Handbook of Magnetic Materials* vol 13, ed K H J Buschow (Amsterdam: Elsevier) pp 229–422